J Dent Sci 2010;5(1):21–29

ORIGINAL ARTICLE

Evaluation of ten extra-alveolar temporary anchorage device insertion sites by cone beam volumetric computer tomography: a pilot study

Yi-Jyun Chen,[1,2] *Chia-Tze Kao,*[2,3] *Tsui-Hsien Huang*[1,2,3]*

[1]College of Oral Medicine, Chung Shan Medical University, Taichung, Taiwan
[2]Department of Orthodontics, Chung Shan Medical University Hospital, Taichung, Taiwan
[3]Institute of Oral Biology and Biomaterial Science, College of Oral Medicine, Chung Shan Medical University, Taichung, Taiwan

Received: Dec 5, 2009
Accepted: Feb 3, 2010

KEY WORDS:
cone beam volumetric computed tomography;
insertion site;
temporary anchorage device

Background/purpose: In order to increase the success rate of temporary anchorage devices (TADs), it is important not to cause root injury or soft-tissue inflammation. The aim of the present study was to evaluate hard- and soft-tissue thicknesses of TAD insertion sites and the perforation ratio with different lengths of TADs by cone beam volumetric computed tomography (CBCT).
Materials and methods: The hard- and soft-tissue thicknesses were evaluated on 10 patients (5 males and 5 females) by CBCT. The ages ranged 20–36 years. Ten regions of interest (ROIs) in extra-alveolar bone were selected and based on anchorage requirements. Soft-tissue depths were measured in the premaxillary and midpalatal regions, while the cortical bone thicknesses were measured in all the other sites. Data were collected and the Wilcoxon rank sum test was used to compare differences, while the Wilcoxon signed rank test was used for paired data.
Results: The average bone depth of the jaw was around 10 mm at most of the extra-alveolar ROIs, except for the infrazygomatic crest and midpalatal region. The average cortical bone thickness of the jaw was around 2 mm. The soft-tissue depth in the premaxillary region was thicker than that of the midpalatal region ($P<0.05$). The infrazygomatic crest possessed the largest variation of hard-tissue depth. The cortical bone thickness increased from the mesial to the distal in both the buccal and lingual areas of the mandible.
Conclusion: CBCT provides better radiographic evaluation than traditional radiographs. TAD insertion at these 10 extra-alveolar sites introduced in the study could be ideal locations. The design of TADs for different ROIs should take hard- and soft-tissue thicknesses into consideration to reduce clinical complications.

Introduction

Since implants are popularly applied as orthodontic anchorage devices,[1–3] miniscrews are applied in various locations in alveolar bone.[4–7] Compared with dental implants and microplates, miniscrews are smaller in size, cheaper, and easier to insert and remove.[8,9] Although there are many benefits of using miniscrews instead of other temporary anchorage devices (TADs), anatomic sites for safe

*Corresponding author. Institute of Oral Biology and Biomaterial Science, College of Oral Medicine, Chung Shan Medical University, 110, Chien-Kuo North Road, Section 1, Taichung 40201, Taiwan.
E-mail: thh@csmu.edu.tw

insertion are still being discussed in recent years.[10–13]

Because of the risk of injuring the root while inserting a miniscrew in the dental alveolar area, many kinds of the insertion guides that are recorded on radiographs were developed.[14–20] Among all of those techniques, some require computed tomography (CT),[21,22] which entails a relatively high cost and increased radiation exposure.[20,23–27]

Recent studies established CT as a useful technology to evaluate intraoral hard tissues and the best location for implant placement.[10,11,13,21,22,28] Advantages of three-dimensional (3D) imaging are numerous.[29] Studies showed that radiation exposure is much lower for cone beam CT (CBCT) than for medical CT, and closer to the range of standard dental film series.[30,31] Presently, although the existing orthodontic patient data were primarily based on two-dimensional (2D) imaging records, CBCT has led to a multitude of clinical applications across all dental disciplines. CBCT data allow measurement of any area in the scanned volume with increased accuracy and without the projection or superimposition errors of 2D techniques; therefore, 3D imaging can provide more-extensive and more-detailed patient evaluations.[32]

Since the inter-alveolar spaces increase in mesiodistal width from the cementoenamel junction to the apical region,[11,33,34] some studies suggested only placing TADs in apical regions, rather than in the cervical region, to decrease the risk of encountering tooth roots.[20,35] However, the best way to prevent root injury is not to insert a miniscrew in the interradicular area, which means the intra-alveolar area.[13]

Extra-alveolar sites for TADs are strongly recommended when considering the risks of encountering tooth roots.[20,33] In addition, TADs in these areas can provide easier and wider applications in tooth movement, such as posterior segment intrusion,[36,37] anterior teeth retraction,[37] impacted second molar uprighting,[38] maxillary molar distal movement,[28,39] and mandibular molar distal movement.[40] TADs in the inter-radicular area can sometimes impede tooth movement, when a tooth has not moved a sufficient distance to an ideal position and is already touching the TAD, a situation that could never occur if the TAD were placed in the extra-alveolar region.

Hard-tissue quality and quantity affect the success rates of TADs.[41] With thin cortical bone and low-density trabecular bone, TAD insertion loading strain values may exceed the level of microfractures, thus leading to screw loosening.[42] Several studies evaluated the cortical bone thickness at various interradicular areas.[10–12,43,44] However, few reports evaluated hard-tissue thicknesses of extra-alveolar areas.[13,45,46]

With CBCT images, we evaluated extra-alveolar sites for TADs. The aim of this study was to evaluate extra-alveolar TAD insertion sites by CBCT. Ten extra-alveolar regions of interest (ROIs) were chosen based on clinical anchorage requirements, with particular emphasis on measuring the cortical bone thickness and acquired bone depth. The perforation ratios with different lengths of TADs were also calculated.

Materials and methods

The craniofacial morphology of 10 adult Taiwanese (5 women and 5 men, with a mean age of 28.7 ± 5.21 years) with no craniofacial anomalies or trauma or systemic diseases was selected from a CBCT (i-CAT imaging system; Imaging Sciences International, Hatfield, PA, USA) databank. The CBCT settings were 120 kVp and a constant-potential voltage waveshape of 3–8 mA. The source-to-sensor distance was 27 inches (68.5 cm) with scan time of 40 seconds and single 360° rotation for image acquisition. The primary reconstruction was 2 minutes, and voxel size was 0.4–0.2 mm. Multi-planar reformatting of those obtained data and ROI measuring were performed with the i-CAT imaging system.

Images of specific regions were simultaneously displayed with their panoramic, axial and sagittal slices so that each specific ROI could be accurately located (Fig. 1). The images were respectively adjusted to the exact tissue threshold of different ROIs. By adjusting the image size, brightness and contrast with i-CAT Vision (Imaging Sciences International), the hard- and soft-tissue margins were definitively marked as shown in Fig. 2.

Ten extra-alveolar ROIs, chosen for the study of hard and soft tissues, were determined by the versatility of clinical use.[13,28,36–40,47] The terminologies for the anatomic ROIs below were based on standard definitions but modified to narrow the ROI for clarity.[13,47] Furthermore, these ROIs were divided into single and dual sites. Single sites, which were located in the anatomic sagittal plane, included the incisive fossa, premaxillary region, midpalatal region, and symphysis. Dual sites, which were located symmetrically on both sides of the coronal plane, included the canine fossa, infrazygomatic (IZ) crest, anterior external oblique ridge (AEOR), retromolar area, and sublingual fossa.

Anatomic ROIs

Maxilla (3 facial and 2 palatal)

The incisive fossa is limited distally by the canine eminence, inferiorly by the apices of the incisors, and superiorly by the nasal cavity (Figs. 2A and 3A).

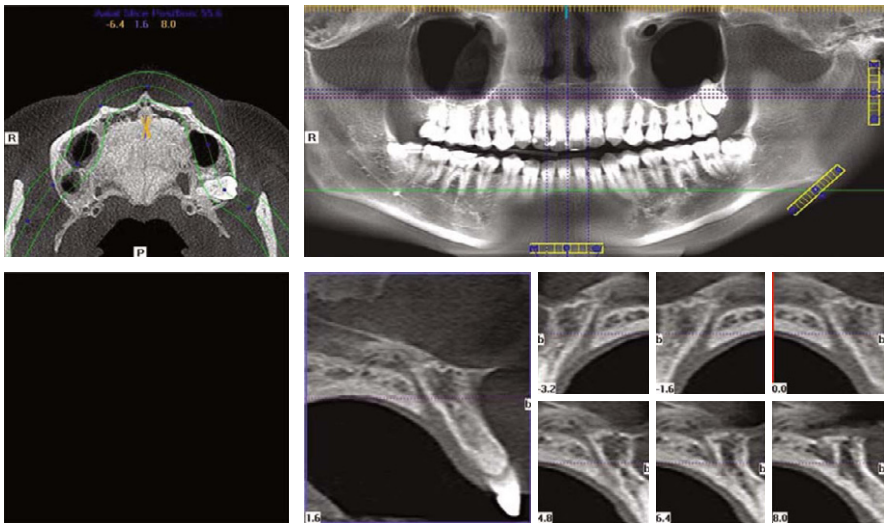

Fig. 1 Specific regions accurately located by software.

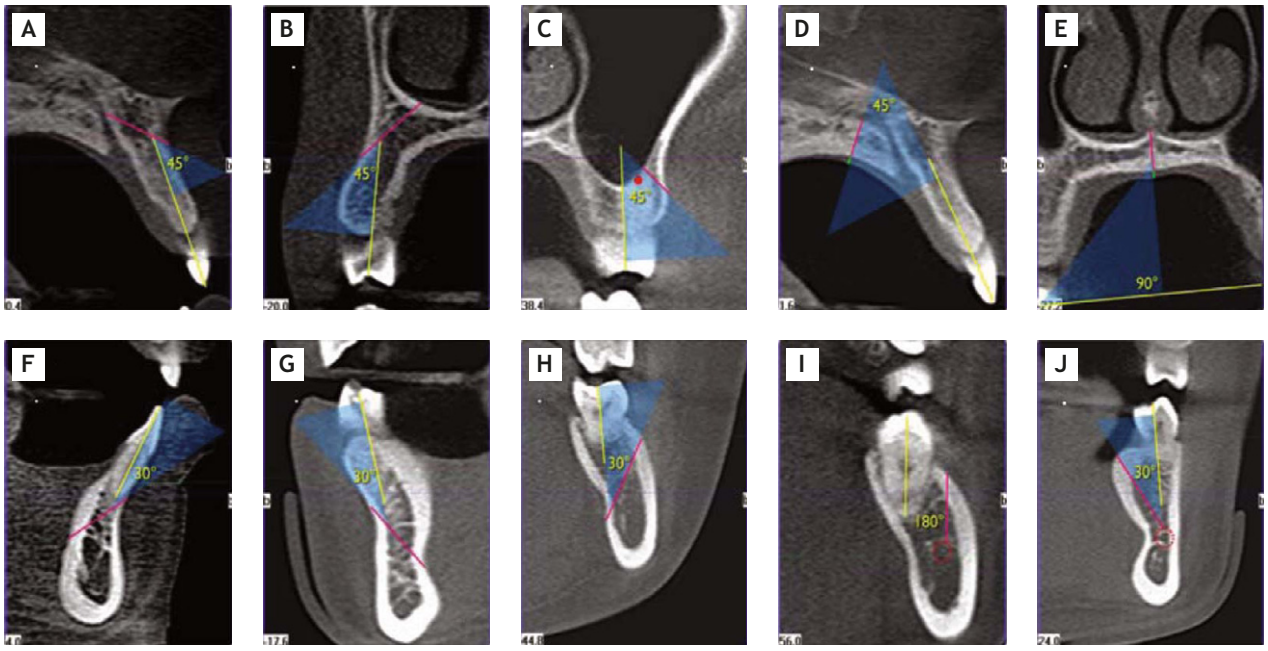

Fig. 2 Computed tomography transaxial section images of the regions of interest. (A) Incisive fossa, (B) canine fossa, (C) infrazygomatic crest, (D) premaxillary region, (E) midpalatal region, (F) symphysis, (G) canine fossa, (H) anterior external oblique ridge, (I) retromolar area, (J) sublingual fossa.

The canine fossa is limited medially by the canine eminence, inferiorly by the apex of the first premolar, and distally by the medial portion of the maxillary sinus (Figs. 2B and 3B). The IZ crest is limited distally by the zygomatic crest, inferiorly by the apex of the mesial root of the first molar, and superiorly by the medial portion of the maxillary sinus and the projecting zygomatic process (Figs. 2C and 3C). The premaxillary region is the paramedial area in the premaxilla region of the palate, limited laterally by the incisors and canine roots and medially by the incisive foramen (Figs. 2D and 3D). The midpalatal region is limited anteroposteriorly between the first and second premolars and mediolaterally by the midpalatal suture (Figs. 2E and 3E).

Mandible (4 facial and 1 lingual)

The symphysis is limited bilaterally by the canine eminences, inferiorly by the mental tubercles, and superiorly by the incisor apices (Figs. 2F and 3F). The canine fossa is limited mesially by the canine eminence, distally by the mental foramen, superiorly by the first premolar apex, and inferiorly by the mandibular inferior border (Figs. 2G and 3G).

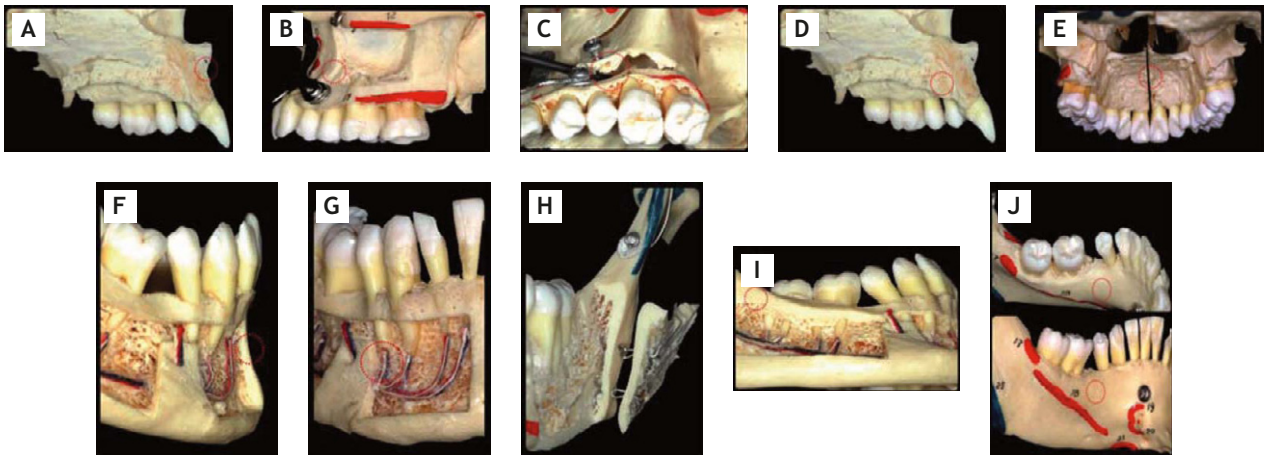

Fig. 3 Anatomic locations of regions of interest. (A) Incisive fossa, (B) canine fossa, (C) infrazygomatic crest, (D) premaxillary region, (E) midpalatal region, (F) symphysis, (G) canine fossa, (H) anterior external oblique ridge, (I) retromolar area, (J) sublingual fossa.

The AEOR is limited laterally by the external oblique ridge and medially by the crestal bone of the second molar (Figs. 2H and 3H). The retromolar area is limited mesially by the distal surface of the second molar, laterally by the external oblique ridge, and superiorly by the ascending ramus (Figs. 2I and 3I). The sublingual fossa is limited anteriorly, posteriorly, and superiorly by the apical portion of the first and second premolar roots (parallel to the tooth long axis) (Figs. 2J and 3J), and inferiorly by the mandibular inferior border.

Measurements

Reference lines for all 10 ROI measurements were established and drawn in transaxial sections at 45° on the maxilla or at 30° on the mandible relative to the long axis of the adjacent teeth, except for the retromolar area and midpalatal region.[47] In the retromolar area, the measurement was taken parallel to the long axis of the adjacent molar (Fig. 2I), while in the midpalatal region, it was taken perpendicular to the occlusal plane (Fig. 2E).

To calibrate the 10 ROI sites for each image, i-CAT Vision software was used. First, the slice control bar, found in various views and positions throughout the program, was dragged to decrease the slice thickness to 0.2 mm. Then, to make a linear measurement, the "Distance" function was selected, and a measurement in millimeters appears in the upper corner of the image. Data were the average of three measurements in the same locations by the same examiner.

Bone depths were measured for all 10 ROIs; in the meanwhile, soft-tissue depths were only quantified in the premaxillary and midpalatal regions, and the cortical bone thicknesses were measured in all other eight sites by CBCT.

Statistical analysis

Descriptive statistics included the mean, standard deviation, and minimum and maximum values, which are listed in Table 1. All statistical analyses were carried out using SPSS version 13.0 (SPSS Inc., Chicago, IL, USA). For each ROI, both the left- and right-side thicknesses (mm) were measured. Comparisons of measurements between sexes were performed with the Wilcoxon rank sum test. The Wilcoxon signed rank test was used for the paired data of labial and lingual cortical bone thicknesses, and for premaxilla and midpalatal soft-tissue thickness comparisons. All values compared with a P value <0.05 were considered to differ statistically and significantly.

Results

The data showed that there were no differences between the right and left sides ($P>0.05$) for bone depth or cortical bone thickness at each ROI. The right and left measurements were, therefore, pooled together for the descriptive statistics (Table 1).

In the comparison between sexes, there were no significant sex differences in most of the measurements, except for the cortical bone thickness of the AEOR and the lingual cortical bone thickness of the symphysis (Table 2). The cortical bone thickness of the AEOR in the male group was thicker than that of the female group ($P=0.009$); in contrast, the lingual cortical bone thickness of the symphysis in the female group was thicker than that of the male group ($P=0.046$).

Among the pairwise comparisons, the soft-tissue thickness of the premaxillary area was significantly thicker than that of the midpalatal area ($P<0.05$);

Table 1. Hard- and soft-tissue thickness measurements for each region of interest (ROI)

ROI	Bone depth (mm)				Cortical bone thickness (mm)			
	Mean	SD	Max	Min	Mean	SD	Max	Min
Maxilla								
Incisive fossa	10.41	2.69	16.2	7.4	1.92	0.33	2.5	1.3
Canine fossa	10.93	3.57	17.0	5.6	2.75	0.67	4.5	1.8
Infrazygomatic crest	5.89	3.92	18.5	3.1	1.96	0.37	3.2	1.4
Premaxillary region	10.21	2.43	14.8	7.2	4.39*	0.58	5.6	3.4
Midpalatal region	6.95	1.25	8.8	4.9	1.37*	0.31	1.7	0.8
Mandible								
Symphysis	12.79	1.6	14.5	9.1	2.11†	0.42	2.8	1.4
Symphysis (labial)					3.91†	0.69	5.0	2.7
Canine fossa	10.19	1.81	13.0	6.9	3.58	0.74	4.9	2.0
Retromolar area	14.73	2.04	17.8	10.4	4.36	1.18	7.0	2.8
Sublingual fossa	11.51	2.07	15.1	8.4	4.27	0.75	5.4	2.9

*Only the soft-tissue thicknesses were measured and compared with each other (P=0.005), not cortical bone depths; †the lingual cortical bone thickness was measured and compared with that of the labial cortex (P=0.005). SD=standard deviation; Min=minimum; Max=maximum.

and the lingual cortex thickness was thicker than that of the labial in the symphysis area ($P<0.05$) (Table 2). The perforation ratios for different TAD lengths are presented in Table 3. No perforation of the maxillary ROI was found when the length of the TAD was 6 mm, except for in the IZ crest area. In the mandibular ROI, the only possible perforation area was the canine fossa area when using an 8-mm TAD.

Discussion

Compared with traditional orthodontic radiographs, CBCT provides images without magnification and superimposition errors, and also 3D imaging and volumetric information. The versatility of CBCT to evaluate hard-tissue availability in an ROI was noted.[45,48] The soft-tissue depth evaluation is recorded by piercing the mucosa with a needle until the attached rubber stop rests on the mucosa.[49,50] By adjusting the tissue threshold, the soft-tissue thickness can be easily measured from the CBCT image with no invasive clinical procedures. The 3D image is reconstructed by discrete data divided into voxels; although inadvertent selection of the nearest neighbor point occurs, a minimal voxel size helps reduce such errors.[51] In addition, the amount of CBCT radiation the patient receives is less than that with other types of tomography.[52]

TAD insertion sites can be divided into two categories: inter-radicular and extra-alveolar areas. Extra-alveolar insertion sites, which can minimize the risks of root injury,[2,34,53] might allow the force direction to be closer to the center of resistance in some situations.[4,18]

Another substantial issue in this study is the TAD insertion angle, which can directly influence the available depth of the hard tissue. Clinically, in order not to cause root injuries, it is easier for clinicians to use the long axis of neighboring teeth as a guide to perform insertion of a TAD. Therefore, all insertion angles for each ROI mentioned in this study were based on previous studies with the neighboring teeth as a guide.[9,13,46]

In the present study, the average bone depths were around or >10 mm, except for the IZ crest and midpalatal region; the average cortical bone thicknesses were around or >2 mm, except for the incisive fossa, IZ crest, and midpalatal region (Table 1). The bone depth of the IZ crest should be at least 6 mm to adequately sustain a miniscrew throughout treatment.[46] The average bone depth of the IZ crest in this study was 5.89 mm; the bone depth of the IZ crest in the male group was longer than 6 mm, but not that in the female group (Table 2). It was supposed that the variation in IZ crest thickness might be due to variations in the maxillary sinus among individuals.[54] There was no sex difference ($P=0.09$) in the cortical bone thickness of the IZ crest.

In a previous study based on 20 Caucasian males, the recommended lengths of the TAD for the maxillary incisive fossa and symphysis differed.[13] The length of the TAD for the symphysis could be longer than that of the incisive fossa in white males. Similar results were also found in our study. The mean bone depth was thicker at the symphysis than the incisive fossa (Table 1).

Table 2. Hard- and soft-tissue thickness measurements in each region of interest (ROI) between sexes

ROI	Bone thickness (mm)									Cortical bone thickness (mm)								
	Male				Female				P	Male				Female				P
	Mean	Max	Min	SD	Mean	Max	Min	SD		Mean	Max	Min	SD	Mean	Max	Min	SD	
Maxilla																		
Incisive fossa	11.30	16.2	7.4	3.68	9.52	11.0	8.5	0.91	0.60	1.74	2.0	1.3	0.30	2.10	2.5	1.8	0.26	0.08
Canine fossa	10.69	17.0	5.6	4.00	11.16	15.6	6.1	3.28	0.92	2.79	4.5	1.8	0.80	2.71	3.8	2.0	0.56	0.67
IZ ridge	7.25	18.5	3.4	5.22	4.52	6.2	3.1	0.99	0.34	2.05	3.2	1.7	0.44	1.86	2.3	1.4	0.29	0.09
Premaxillary region*	9.50	11.8	7.5	1.97	10.92	14.8	7.2	2.86	0.47	4.68	5.6	4.1	0.58	4.10	4.7	3.4	0.47	0.11
Midpalatal region*	6.66	8.8	4.9	1.56	7.24	8.4	6.1	0.93	0.46	1.24	1.6	0.8	0.30	1.50	1.7	1.0	0.28	0.13
Mandible																		
Symphysis	12.98	14.5	11.2	1.30	12.60	14.1	9.1	1.99	0.92	1.96	2.3	1.4	0.38	2.26	2.8	1.7	0.44	0.40
Symphysis (L)†										3.50	4.3	2.7	0.60	4.32	5.0	3.7	0.54	0.046
Canine fossa	10.98	13.0	8.7	1.44	9.40	12.8	6.9	1.85	0.17	3.87	4.9	2.8	0.74	3.29	4.0	2.0	0.65	0.53
AEOR	14.00	16.4	12.0	1.68	12.48	13.9	9.5	1.19	0.14	4.33	5.1	3.3	0.58	3.59	4.8	2.7	0.55	0.009
Retromolar area	15.67	17.6	13.2	1.37	13.78	17.8	10.4	2.21	0.11	4.78	7.0	3.6	1.40	3.94	4.8	2.8	0.78	0.45
Sublingual fossa	10.84	13.3	8.4	1.81	12.18	15.1	9.3	2.19	0.60	4.37	5.4	2.9	0.75	4.16	5.1	3.1	0.77	0.29

*Only the soft tissue thicknesses were measured, not the cortical bone depths; †lingual cortical bone thickness was measured. SD=standard deviation; Max=maximum; Min=minimum; IZ=infrazygomatic; AEOR=anterior external oblique ridge.

Table 3. Numbers and ratio of perforations for incremental length of the temporary anchorage devices

ROI	4 mm		6 mm		8 mm		10 mm		12 mm	
	No.	%	No.	%	No.	%	No.	%	No.	%
Maxilla										
Incisive fossa*	0/10	0	0/10	0	1/10	10	6/10	60	8/10	80
Canine fossa†	0/20	0	1/20	5	5/20	25	9/20	45	11/20	55
Infrazygomatic crest†	6/20	30	16/20	80	18/20	90	18/20	90	18/20	90
Premaxillary region*	0/10	0	0/10	0	3/10	30	5/10	50	8/10	80
Midpalatal region*	0/10	0	2/10	20	8/10	80	10/10	100	10/10	100
Mandible										
Symphysis*	0/10	0	0/10	0	0/10	0	1/10	10	2/10	20
Canine fossa†	0/20	0	0/20	0	2/20	10	9/20	45	17/20	85
AEOR†	0/20	0	0/20	0	0/20	0	1/20	5	3/20	15
Retromolar area†	0/20	0	0/20	0	0/20	0	0/20	0	3/20	15
Sublingual fossa†	0/20	0	0/20	0	0/20	0	5/20	25	13/20	65

*Single sites; †dual sites, including both right and left sides. AEOR = anterior external oblique ridge.

The cortical bone thickness of the lingual symphysis and AEOR showed a significant difference between sexes. The female lingual symphysis cortex was thicker than that of males, whereas males had a thicker cortex in the AEOR (Table 2). A recent study also reported that the cortex was thinner in females than in males in the posterior buccal regions.[55]

To adequately sustain a TAD throughout treatment, a mechanical lock is needed, rather than bone integration as with dental implants. The amount of cortical bone in contact with the TAD threads plays an important role in mechanical locking.[56] Furthermore, this mechanical lock can be either a unicortical or bicortical anchorage. A unicortical anchorage means that the TAD penetrates only one cortical plate, whereas with bicortical anchorage, the TAD is long enough to penetrate two cortical plates. For example, if the TAD is long enough, it can penetrate the buccal cortical plate and bone marrow and embed into the lingual cortical plate at the symphysis. Clinically, it is important for clinicians to be familiar with the anatomy of TAD insertion sites. When a unicortical anchorage is needed, a TAD length of up to 10 mm is not recommended for all ROIs, except in the retromolar area. As for bicortical anchorage, the clinician must know the exact bone depth to prevent soft-tissue perforation on the opposite side.

As to soft-tissue concerns, TADs are inserted in the keratinized gingival tissue area and designed with a smooth neck for most applications.[9] However, placing a TAD in some extra-alveolar areas could potentially cause mucosal inflammation. Although a specially designed appliance was used to prevent associated problems, a complicated design can cause food impaction and discomfort.[13] Another way to prevent inflammation is to place the TAD in the mobile mucosa, that is, cover the screw head beneath the mucosa with an extension for force application. In the presented results, the premaxillary soft tissue was statistically thicker than that of the midpalate, showing that a TAD with a longer smooth neck design should be considered in the premaxillary region.

In conclusion, CBCT provides a better clinical evaluation than traditional radiographs. The results validate these 10 extra-alveolar regions as being safe host sites for a TAD. In order to reduce the risks of perforation, different lengths of TADs ranging 6–10 mm are recommended for these 10 ROIs. The soft tissue depth in the palatal area is thicker in the premaxillary than the midpalatal region. The design of TADs for different ROIs should take both hard- and soft-tissue thicknesses into considerations to reduce clinical complications. As for the length selection of TADs, individual evaluation should be of concern to clinicians.

References

1. Roberts WE, Nelsen CL, Goodacre CJ. Rigid implant anchorage to close a mandibular first molar extraction site. *J Clin Orthod* 1994;38:693–704.
2. Umemori M, Sugawara J, Mitani H, Nagasaka H, Kawamura H. Skeletal anchorage system for open-bite correction. *Am J Orthod Dentofacial Orthop* 1999;115:166–74.
3. Kuroda S, Katayama A, Takano-Yamamoto T. Severe anterior open-bite case treated using titanium screw anchorage. *Angle Orthod* 2004;74:558–67.
4. Costa A, Raffainl M, Melsen B. Miniscrews as orthodontic anchorage: a preliminary report. *Int J Adult Orthodon Orthognath Surg* 1998;13:201–9.
5. Kanomi R. Mini-implant for orthodontic anchorage. *J Clin Orthod* 1997;31:763–7.

6. Park YC, Lee SY, Kim DH, Jee SH. Intrusion of posterior teeth using mini-screw implants. *Am J Orthod Dentofacial Orthop* 2003;123:690–4.
7. Park HS, Kwon DG, Sung JH. Nonextraction treatment with microscrew implant. *Angle Orthod* 2004;74:539–49.
8. Melsen B, Costa A. Immediate loading of implants used for orthodontic anchorage. *Clin Orthod Res* 2000;3:23–8.
9. Melsen B. Mini-implants: where are we? *J Clin Orthod* 2005; 39:539–47.
10. Deguchi T, Nasu M, Murakami K, Yabuuchi T, Kamioka H, Takano-Yamamoto T. Quantitative evaluation of cortical bone thickness with computed tomographic scanning for orthodontic implants. *Am J Orthod Dentofacial Orthop* 2006; 129:721.e7–12.
11. Poggio PM, Incorvati C, Velo S, Carano A. "Safe zones": a guide for miniscrew positioning in the maxillary and mandibular arch. *Angle Orthod* 2006;76:191–7.
12. Kim HJ, Yun HS, Park HD, Kim DH, Park YC. Soft-tissue and cortical-bone thickness at orthodontic implant sites. *Am J Orthod Dentofacial Orthop* 2006;130:177–82.
13. Costa A, Pasta G, Bergamaschi G. Intraoral hard and soft tissue depths for temporary anchorage devices. *Semin Orthod* 2005;11:10–5.
14. Cousley RR, Parberry D. Surgical stents for accurate miniscrew insertion. *J Clin Orthod* 2006;40:412–7.
15. Barros SE, Janson G, Chiqueto K, Freitas M, Henriques J, Pinzan A. A three-dimensional radiographic-surgical guide for mini-implant placement. *J Clin Orthod* 2006;40: 548–54.
16. Bae SM, Park HS, Kyung HM, Kwon OW, Sung JH. Clinical application of micro-implant anchorage. *J Clin Orthod* 2002; 36:298–302.
17. Kyung SH, Choi JH, Park YC. Miniscrew anchorage used to protract lower second molars into first molar extraction sites. *J Clin Orthod* 2003;37:575–9.
18. Carano A, Velo S, Leone P, Siciliani G. Clinical applications of the Miniscrew Anchorage System. *J Clin Orthod* 2005;39:9–24.
19. Maino BG, Bednar J, Pagin P, Mura P. The spider screw for skeletal anchorage. *J Clin Orthod* 2003;37:90–7.
20. Kyung HM, Park HS, Bae SM, Sung JH, Kim IB. Development of orthodontic micro-implants for intraoral anchorage. *J Clin Orthod* 2003;37:321–8.
21. Kitai N, Yasuda Y, Takada K. A stent fabricated on a selectively colored stereolithographic model for placement of orthodontic mini-implants. *Int J Adult Orthodon Orthognath Surg* 2002;17:264–6.
22. Freudenthaler JW, Haas R, Bantleon HP. Bicortical titanium screws for critical orthodontic anchorage in the mandible: a preliminary report on clinical applications. *Clin Oral Implants Res* 2001;12:358–63.
23. Sato S, Arai Y, Shinoda K, Ito K. Clinical application of a new cone-beam computerized tomography system to assess multiple two-dimensional images for the preoperative treatment planning of maxillary implants: case reports. *Quintessence Int* 2004;35:525–8.
24. Clark DE, Danforth RA, Barnes RW, Burtch ML. Radiation absorbed from dental implant radiography: a comparison of linear tomography, CT scan, and panoramic and intraoral techniques. *J Oral Implantol* 1990;16:156–64.
25. Ekestubbe A, Thilander A, Grondahl K, Grondahl HG. Absorbed doses from computed tomography for dental implant surgery: comparison with conventional tomography. *Dentomaxillofac Radiol* 1993;22:13–7.
26. Lecomber AR, Yoneyama Y, Lovelock DJ, Hosoi T, Adams AM. Comparison of patient dose from imaging protocols for dental implant planning using conventional radiography and computed tomography. *Dentomaxillofac Radiol* 2001;30: 255–9.
27. Ngan DC, Kharbanda OP, Geenty JP, Darendeliler MA. Comparison of radiation levels from computed tomography and conventional dental radiographs. *Aust Orthod J* 2003; 19:67–75.
28. Crismani AG, Bernhart T, Bantleon HP, Cope JB. Palatal implants: the Straumann Orthosystem. *Semin Orthod* 2005; 11:16–23.
29. Mah J, Hatcher DC. Current status and future needs in craniofacial imaging. *Orthod Craniofac Res* 2003;6(Suppl 1): 10–6.
30. Mah JK, Danforth RA, Bumann A, Hatcher D. Radiation absorbed in maxillofacial imaging with a new dental computed tomography device. *Oral Surg Oral Med Oral Pathol Oral Radiol Endod* 2003;96:508–13.
31. Ludlow JB, Davies-Ludlow LE, Brooks SL. Dosimetry of two extraoral direct digital imaging devices: NewTom cone beam CT and Orthophos Plus DS panoramic unit. *Dentomaxillofac Radiol* 2003;32:229–34.
32. Hung J, Bumann A, Mah J. Three-dimensional radiographic analysis in orthodontics. *J Clin Orthod* 2005;39:421–8.
33. Borah GL, Ashmead D. The fate of teeth transfixed by osteosynthesis screw. *Plast Reconstr Surg* 1996;97:726–9.
34. Lee KJ, Joo E, Kim KD, Lee JS, Park YJ, Yu HS. Computed tomographic analysis of tooth-bearing alveolar bone for orthodontic miniscrew placement. *Am J Orthod Dentofacial Orthop* 2009;135:486–94.
35. Costa A, Levrini L, Tagliabue A. Osteointegrazione negli impianti come ancoraggio ortodontico. *Ital J Oral Implantol* 2000;2:133–9.
36. Xun C, Zeng X, Wang X. Microscrew anchorage in skeletal anterior open-bite treatment. *Angle Orthod* 2007;77: 47–56.
37. Melsen B, Verna C. Miniscrew implants: the Aarhus anchorage system. *Semin Orthod* 2005;11:24–31.
38. Giancotti A, Arcuri C, Barlattani A. Treatment of ectopic mandibular second molar with titanium miniscrews. *Am J Orthod Dentofacial Orthop* 2004;126:113–7.
39. Kinzinger GS, Diedrich PR, Bowman SJ. Upper molar distalization with a miniscrew-supported distal jet. *J Clin Orthod* 2006;40:672–8.
40. Sugawara J, Daimaruya T, Umemori M, et al. Distal movement of mandibular molars in adult patients with the skeletal anchorage system. *Am J Orthod Dentofacial Orthop* 2004; 125:130–8.
41. Dalstra M, Cattaneo PM, Melsen B. Load transfer of miniscrews for orthodontic anchorage. *Orthodontics* 2004;1: 53–62.
42. Frost HM. Perspectives: bone's mechanical usage windows. *Bone Miner* 1992;19:257–71.
43. Jonasson G, Kiliaridis S, Gunnarsson R. Cervical thickness of the mandibular alveolar process and skeletal bone mineral density. *Acta Odontol Scand* 1999;57:155–61.
44. Sarikaya S, Haydar B, Ciğer S, Ariyürek M. Changes in alveolar bone thickness due to retraction of anterior teeth. *Am J Orthod Dentofacial Orthop* 2002;122:15–26.
45. King KS, Lam EW, Faulkner MG, Heo G, Majore PW. Vertical bone volume in the paramedian palate of adolescents: a computed tomography study. *Am J Orthod Dentofacial Orthop* 2007;132:783–8.
46. Liou EJ, Chen PH, Wang YC, Lin JC. A computed tomographic image study on the thickness of the infrazygomatic crest of the maxilla and its clinical implications for miniscrew insertion. *Am J Orthod Dentofacial Orthop* 2007;131:352–6.
47. Moore KL. The head. In: Moore KL, ed. *Clinically Oriented Anatomy*, 2nd ed. Baltimore: Williams & Wilkins, 1985: 794–982.
48. Siwerdsen JH, Jaffray DA. Cone-beam computed tomography with a flat-panel imagery. *Med Phys* 1999;26:2635–47.

49. Wara-aswapati N, Pitiphat W, Chandrapho N, Rattanayatikul C, Karimbux N. Thickness of palatal masticatory mucosa associated with age. *J Periodontol* 2001;72:1409–12.
50. Schulze R, Curiè D, d'Hoedt B. B-mode versus A-mode ultrasonographic measurements of mucosal thickness in vivo. *Oral Surg Oral Med Oral Pathol* 2002;93:1.
51. Patera J. *Iso-surface Extraction and Approximation Error* (Technical Report DCSE/TR-2004-15). Plzen, Czek Republic: Centre of Computer Graphics and Data Visualisation, Department of Computer Science and Engineering, University of West Bohemia, 2004.
52. Mozzo P, Procacci C, Tacconi A, Martini PT, Andreis IA. A new volumetric CT machine for dental imaging based on the cone beam technique: preliminary results. *Eur Radiol* 1998;8:1558–64.
53. Ohmae M, Saito S, Morohashi T, et al. A clinical and histological evaluation of titanium mini-implants as anchors for orthodontic intrusion in the beagle dog. *Am J Orthod Dentofacial Orthop* 2001;119:489–97.
54. Eberhardt JA, Torabinejad M, Christiansen EL. A computed tomographic study of the distances between the maxillary sinus floor and the apices of the maxillary posterior teeth. *Oral Surg Oral Med Oral Pathol Oral Radiol Endod* 1992;73:345–7.
55. Ono A, Motoyoshi M, Shimizu N. Cortical bone thickness in the buccal posterior region for orthodontic mini-implants. *Int J Oral Maxillofac Surg* 2008;37:334–40.
56. Monnerat C, Restle L, Mucha JN. Tomographic mapping of mandibular interradicular spaces for placement of orthodontic mini-implants. *Am J Orthod Dentofacial Orthop* 2009; 135:428–9.